CHEMISTRY
A EUROPEAN JOURNAL

DOI: 10.1002/chem.200701541

Preparation and Properties of Proteinaceous Microspheres Made Sonochemically

Aharon Gedanken*[a]

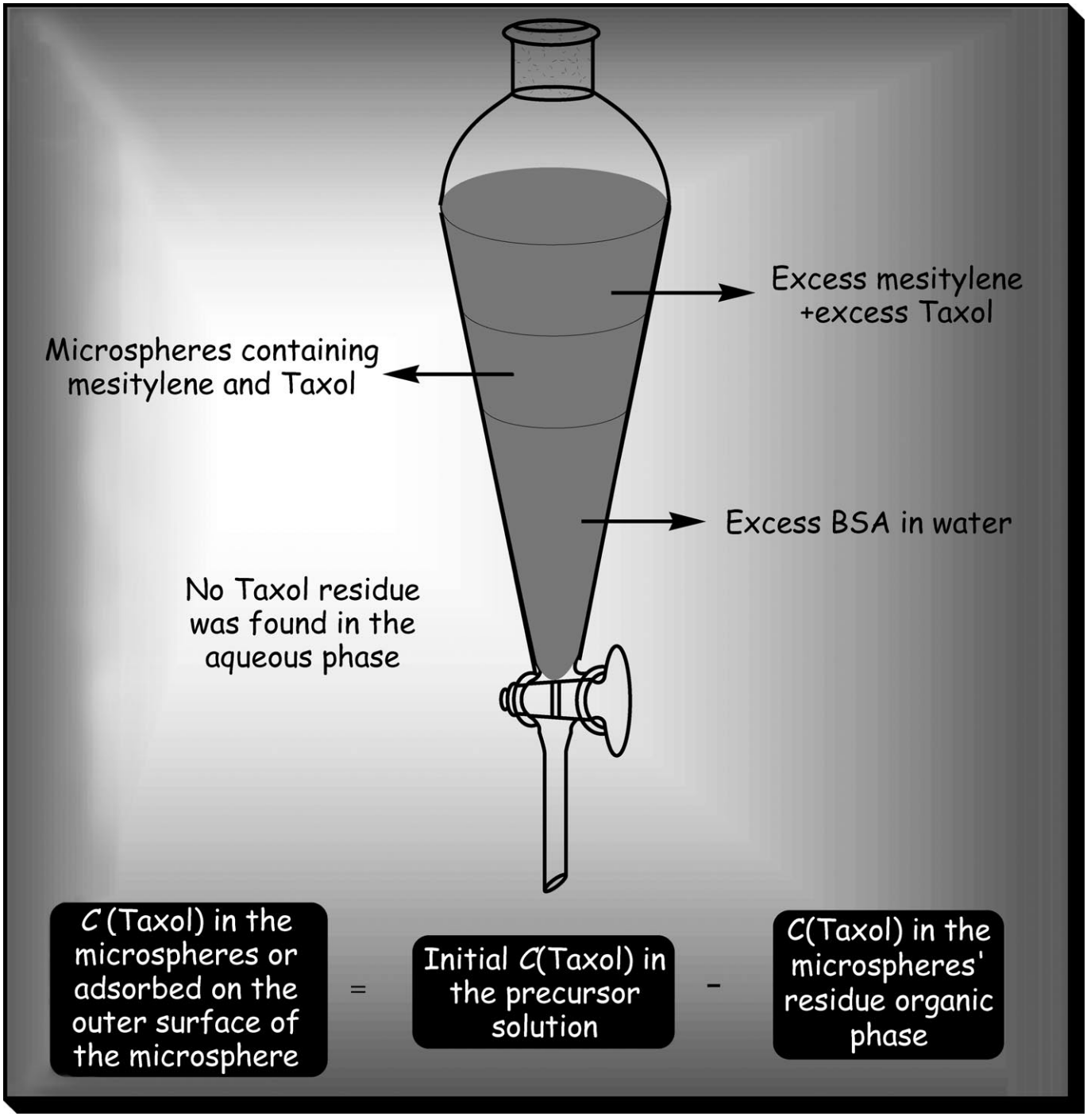

Abstract: In 1990, Suslick and co-workers developed a method in which they used high-intensity ultrasound to make aqueous suspensions of proteinaceous microcapsules filled with water-insoluble liquids, and demonstrated the chemical mechanism of their formation.[1] Suslick's paper opened up a new field that is reviewed in the current manuscript, and this article will attempt to review the experiments that have been conducted since the discovery of this phenomenon. It will answer questions regarding the mechanism of the formation of the microspheres, whether the sonication denaturates the protein or if its biological activity is maintained, and, finally, will address possible applications of the proteinaceous microspheres. Proteinaceous microbubbles will be referred to as proteinaceous microspheres (PM) throughout this review, although they may not have a perfect spherical shape in all cases. This review will start with a short introduction to sonochemistry, although this topic is, and has been reviewed frequently.[2–7] The review covers literature published until December 2006.

Keywords: drug encapsulation · microspheres · nanoparticles · proteins · sonochemistry

Sonochemistry

Sonochemistry is the research area in which molecules undergo chemical reaction due to the application of powerful ultrasound radiation (20 KHz–10 MHz).[2] The physical phenomenon responsible for the sonochemical process is acoustic cavitation. Let us first address the question of how 20 kHz radiation can rupture chemical bonds (this question also relates to 1 MHz radiation), and try to explain the role of a few parameters in determining the yield of a sonochemical reaction, and then describe the unique products obtained when ultrasound radiation is used in materials science.

A number of theories have been developed to explain how 20 kHz ultrasonic radiation can break chemical bonds, and they all concur that the main event in sonochemistry is the creation, growth, and collapse of a bubble that is formed in the liquid. The first question is how such a bubble can be formed, considering the fact that the forces required to separate water molecules to a distance of two van der Waals radii would require a power of $10^5\,W\,cm^{-1}$?[2] On the other hand, it is known that in a sonication bath, with a power of $0.3\,W\,cm^{-1}$,[2] water is readily converted into hydrogen peroxide. Different explanations have been offered; they are all based on the existence of unseen particles, or gas bubbles, that decrease the intermolecular forces, enabling the creation of the bubble. The experimental evidence for the importance of unseen particles in sonochemistry is that when the solution undergoes ultrafiltration, before the application of the ultrasonic power there is no chemical reaction and chemical bonds are not ruptured. The second stage is the growth of the bubble, which occurs through the diffusion of solute vapor into the volume of the bubble. The third stage is the collapse of the bubble, which occurs when the bubble size reaches its maximum value. From here we will adopt the hot-spot mechanism, one of the theories that explain why, upon the collapse of a bubble, chemical bonds are broken. This theory claims that very high temperatures (5000–25 000 K)[8] are obtained upon the collapse of the bubble. Since this collapse occurs in less than a nanosecond,[8,9] very high cooling rates, in excess of $10^{11}\,K\,s^{-1}$, are obtained. This high cooling rate hinders the organization and crystallization of the products. For this reason, in all cases dealing with volatile precursors in which gas-phase reactions are predominant, amorphous nanoparticles are obtained. The sonochemical reaction can be a gas-phase reaction involving usually the vapors of the volatile reactants. In this case, the reaction takes place at very high temperatures of about 5000 K. If, on the other hand, the precursor is a nonvolatile compound, the reaction occurs in a 200 nm ring surrounding the collapsing bubble.[10] In this case, the sonochemical reaction occurs in the liquid phase.

The Sonochemical Synthesis of Proteinaceous Microspheres

Air-filled proteinaceous microspheres (PM) were synthesized by sonication prior to Suslick's work. For example, air-filled human serum albumin were made by Dick and Feinstein[11,12] as contrast agents in echosonography. These products suffer from short storage life, low microbubble stability, or high toxicity.[11–14] The first liquid-filled proteinaceous microspheres (PM) were prepared by Suslick.[1] They were made of BSA (bovine serum albumin) and were filled with *n*-dodecane, *n*-decane, *n*-hexane, cyclohexane, or toluene. The synthesis was conducted under high-intensity ultrasonic probe and 1.5×10^9 microcapsules per mL were obtained upon sonicating the precursor solution under air or O_2. The average diameter of the PM was 2.5 μm with a narrow size distribution (Gaussian distribution $=\pm1.0$ μm). Ultrasonic irradiation of human serum albumin (HSA) generates similar

[a] Prof. A. Gedanken
Department of Chemistry and Kanbar Laboratory for Nanomaterials
Bar-Ilan University Center for Advanced Materials
and Nanotechnology
Bar-Ilan University, Ramat-Gan 52900 (Israel)
Fax: (+972) 3-5351250
E-mail: gedanken@mail.biu.ac.il

microcapsules to those of the BSA; the same is true for the PM of hemoglobin (Hb).[1]

To investigate the microcapsule's interior, water-insoluble 5,10,15,20-tetraphenylporphyrin (H_2TPP) was used as a probe. H_2TPP is soluble in a wide range of medium-polarity liquids, but is completely insoluble in water or aqueous protein solutions.[1] These measurements showed that although these protein microcapsules are suspended in water, a nonaqueous liquid is present inside. The first question raised by Suslick and co-workers was how are the microcapsules formed and what holds them together?[1] The answer to this question relates also to the importance of the nonoaqueous liquid. Emulsification must occur during the microscopic dispersion of the nonaqueous phase into the aqueous protein solution.

Ultrasonic emulsification is a well-known process and does occur in this biphasic system. Emulsification is necessary for microcapsule formation. However, if vortex mixing emulsification is used instead, microcapsules are not formed. Consequently, emulsification by itself is not sufficient for microsphere formation. Thermal or solvent denaturation (for which O_2, N_2, and Ar should give similar results) cannot explain the microcapsule permanence. Because Suslick found that PMs are created only in O_2 or air, the answer must involve the chemistry associated with ultrasound radiation. Aqueous sonochemistry caused by the implosive collapse of bubbles produces $OH^{\bullet}$ and $H^{\bullet}$.[15] The radicals so-produced form H_2, H_2O_2, and, in the presence of O_2, superoxide $HO_2^{\bullet}$.[16,17] Hydroxyl, superoxide, and peroxide radicals are all potential protein cross-linking agents. Using various trapping agents, they concluded[1] that the important oxidant involved in microcapsule formation is superoxide. They proposed that the cysteine, which is present in BSA, HSA, and Hb, is oxidized by the superoxide radical. The microcapsules are held together by protein cross-linking through disulfide linkages from cysteine oxidation. Myoglobin (Mb), which has no cysteine, revealed a substantial decrease in microcapsule yield relative to Hb.

The employment of a protein disulfide cleavage reagent, such as dithioerythritol, destroyed the PM. In a similar way, inhibiting the oxidation of cysteine by alkylation with *N*-ethylmaleimide reduced the formation of PM considerably. In a later publication, Suslick and Grinstaff[18] reported on the preparation of aqueous suspensions of air-filled proteinaceous microbubbles. The synthesis involves the ultrasonic irradiation of aqueous protein solutions in the presence of O_2. Yields and size distribution of human and BSA microbubbles were determined as a function of various experimental parameters. The ultrasound irradiation was conducted at 50 °C and lasted three minutes.[18] This irradiation time is typical for the optimal formation of the PM. If longer irradiation times are used, a reduction in the number of PM is observed. It is worth mentioning[19] that the difference in the formation of the liquid- and air-filled bubbles is in the position of the sonicator. In a typical synthesis of liquid-filled PM, the organic liquid is layered over a 5% w/v protein solution and the horn is positioned at the organic–water interface. For air-filled microbubbles, the horn is placed at the air–water interface.[19] The chemical nature of these microbubbles and the origin of their remarkably long lifetimes have been explored. The microbubbles are held together primarily by interprotein cross-linking of cysteine residues. The principal cross-linking agent is superoxide, created by the extremely high temperatures produced during acoustic cavitation.

Are Proteinaceous Microspheres Biologically Active?

Suslick has addressed this question in the microspheres formed with hemoglobin (Hb).[20] The microbubbles of Hb were filled with air and are described as having many of the ideal characteristics needed for use as a blood substitute. As a blood substitute, they have to fully bind oxygen in the lungs and efficiently unload oxygen in the tissues, which implies positive cooperativity in oxygen binding. Second, it should respond to the body's own allosteric effectors (such as phosphates) to modify its binding properties in vivo in response to metabolic needs. Third, the blood substitute must possess adequate oxygen-carrying capacities. Fourth, it must not trigger any immunogenic response or damage the kidneys or other organs. Fifth, the blood substitute must be stable under storage conditions.[20] Indeed, as far as the last condition is concerned, the Hb microbubbles have excellent stability and show minimal degradation ($<25\%$) after storage for six months at 4 °C. The microbubbles are initially in met-Fe^{III} form, which cannot bind O_2; hence, for the iron reduction to Fe^{II}, Suslick and Wong[20] used the Hyashi process.[21] Before each oxygen binding experiment, the reduction system was added to the microbubbles and left at 4 °C for 24–36 h and then removed by centrifugal filtration. Oxygen binding curves for native Hb and the microbubbles were determined by using an apparatus similar to that described by Imai and co-workers.[22] The absorption spectra of the microbubbles of met-Fe^{III}, oxy-Fe^{II}, and deoxy-Fe^{II} have their intense peak in the 400–450 nm range (Soret bands), and weak absorption bands in the 550–600 nm region.[20] The

Aharon Gedanken obtained his M.Sc. from Bar-Ilan University, and his Ph.D. degree from Tel Aviv University, Israel. After postdoctoral positions at USC in Los Angeles, he returned to Bar-Ilan in Pct. 1975 as a senior faculty member. He has published over 450 scientific papers and has filed more than 15 patents. Prof. Gedanken has a research group consisting of about 25 students, including several postdocs.

absorption bands of the native Hb appear in the same region. This indicates that the environment surrounding the active heme site has not been altered significantly during the microsphere formation process. The results of the oxygen binding have shown that the $P_{1/2}$ value (the partial pressure of oxygen at which half of the available binding sites on Hb are bound to O_2) are similar to the native Hb and sonicated Hb microbubbles.[20] This means that the microtubules can bind and release oxygen at the same oxygen pressures as native Hb. A surprising result obtained by Suslick and co-workers[20] was related to the Hill coefficient (indicating the level of cooperativity between oxygen binding sites). The Hill coefficient of the microbubbles was significantly higher than that of the native Hb solution.

Allostric effectors of native Hb, such as inositol hexaphosphate, have shown a similar activity for the Hb microbubbles. The authors have calculated the oxygen-carrying capacity of the Hb microbubbles and found that for O_2 filled microbubbles it is greater by 50% than whole blood (0.32 mL O_2 per mL microbubble versus 0.2 mL O_2 per mL blood).[20] Two other investigations probing the biological activity of PMs were conducted in Gedanken's group.[23,24] In the first, avidin microspheres were prepared by using the sonochemical method. It was found that these microspheres can bind biotin, but to a lesser degree than the native protein. It is known that the complex formed between the vitamin biotin and avidin is the strongest interaction known between a ligand and a protein.[25] The most important bonds in the binding of biotin to avidin are the hydrogen bonds formed between the carbonyl group on the ureido ring of biotin and the single tyrosine (Tyr-33) in avidin. The activity of the biotin binding sites in the microspherical avidin (MCAV) was checked after the sonochemical reaction, by using the dye 4′-hydroxyazobezene-2-carboxylic acid (HABA), as mentioned in reference [26]. HABA binds to avidin and is removed by the addition of biotin. The binding of HABA by avidin is accompanied by spectral changes that can be observed by the naked eye when the color changes from yellow to red. This biotin-binding assay was used to prove the MCAV binding capabilities to biotin. This was part of a general approach to check whether the microspherical protein remains with the same biological activity as the native protein. Neither a change of color, nor the appearance of an absorption peak at 500 nm, characteristic of the presence of the avidin–HABA complex, were detected. To find whether avidin microspheres bind biotin, a more sensitive method using a biotin-labeled peroxidase[27] was employed. This labeled biotin is known to bind avidin and to undergo a color change (transparent to blue), which is easily detected by the naked eye. As mentioned above, this experiment yielded positive results, namely, indicating that MCAV binds biotin. The peroxidase can be attached to avidin microspheres only through the biotin residue. This measurement is the first proof that avidin microspheres can bind biotin. Another proof of this conclusion is obtained by using the TPD (temperature-programmed desorption) technique coupled with mass spectrometry (MS). In this method, the sample is heated in a mass spectrometer and the species removed from a sample are detected by MS as a function of temperature. Avidin microspheres, which were first treated with biotin,[28] were heated in the MS over a temperature range of 25–400 °C at a rate of 10 °C min^{-1}. For comparison, a control experiment with avidin microspheres only was also performed. In Figure 1, the MS of the avidin-microsphere–

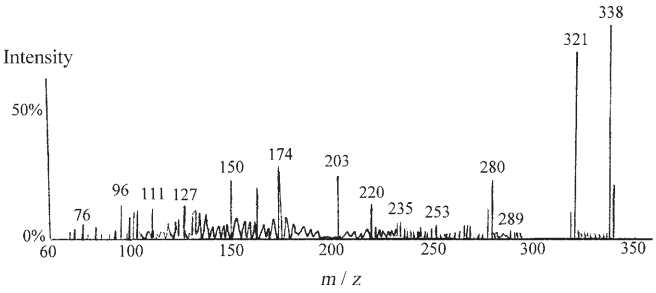

Figure 1. Mass spectrometry (MS) analysis of the avidin microspheres treated with biotin, at 160 °C.

biotin complex at 160 °C is presented. Strong peaks at m/z 321 and 338 were detected. The peak at an atomic mass unit (amu) of 321 can be assigned to a residue containing a biotin molecule bound to a phenyl group. The second peak at 338 was attributed to the addition of an ammonia molecule bound to the former species, because these experiments were conducted under a flow of ammonia. When identical measurements was carried out at 300 °C, the MS of the avidin-microsphere–biotin complex yielded a strong peak at m/z 245, which was attributed to (biotin)H^+. These results show that at a lower temperature (160 °C), the fragmentation occurred in the skeleton of the microspheres and the origin of phenyl group was in the avidin. On the other hand, a much higher temperature (300 °C) is required to break the bond between the PM of avidin and biotin. These results indicate clearly that despite the negative results obtained by the HABA test, the microspherical avidin binds biotin. To further substantiate this conclusion, and to provide some quantitative measure as to the amount of biotin bonded to the avidin microspheres, TGA (thermal gravimetric analysis) experiments were conducted. In Figure 2 the TGA results of the microspherical avidin–biotin complex are illustrated; the TGA of the corresponding native avidin–biotin complex is also shown. The samples were heated under a flow of N_2, while the heating rate was 10 °C min^{-1}. A weight loss of 50% was measured in the 30–500 °C temperature range for the avidin-microsphere–biotin complex, while a weight loss of 70% was detected for the native avidin–biotin complex. There is no doubt that biotin is bound to avidin in both cases. Moreover, since in both cases the weight loss starts at 240 °C, the major part of weight loss can be attributed to biotin and not to the solvents. It can therefore be concluded that biotin is bonded to the avidin microspheres. The dissociation temperature in both figures is also informative. It is known that hydrogen bonds play a major

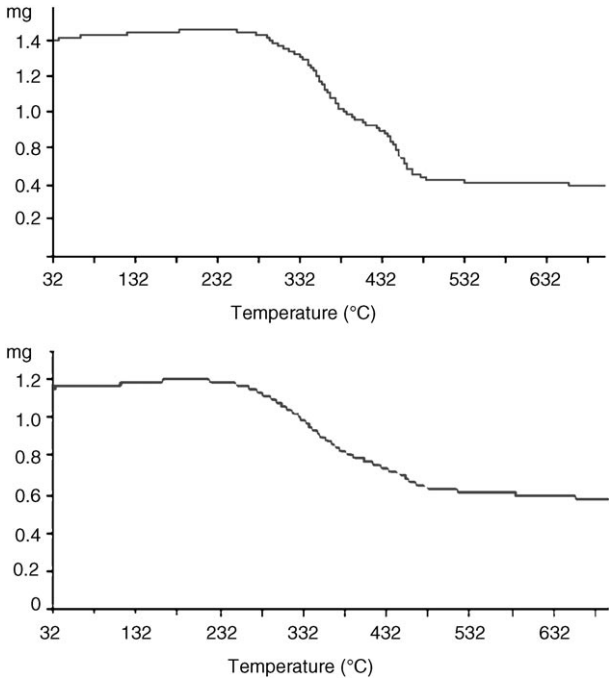

Figure 2. TGA analysis of the native avidin (top) and avidin microspheres (bottom) treated with biotin. Heating rate was 10 °C min^{-1} under a flow of N_2.

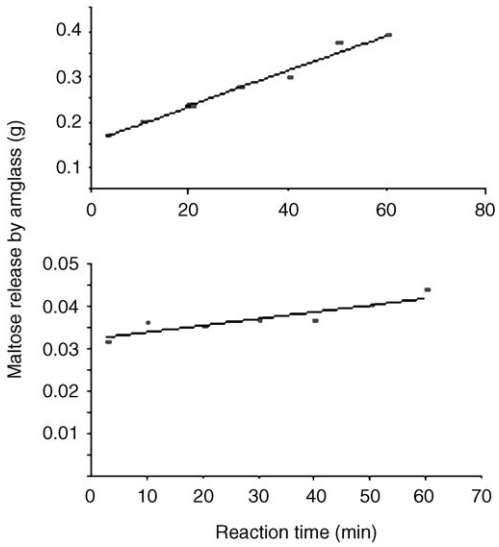

Figure 3. Top: Released maltose versus reaction time by the big microspheres. (Prepared from 0.05 % w/v of amylase). Bottom: Released maltose versus reaction time by the small microspheres (prepared from 0.017 % w/v of amylase).

role in the binding of biotin to native avidin. The shape of the TGA curves, and the temperature at which the weight loss is detected, are almost identical for native avidin and microspherical avidin bound to biotin. This result indicates that the same binding scheme operates for native and microspherical-avidin–biotin complexes.

In a second study related also to the biological activity of PMs, Avivi[24] formed microspheres of α-amylase (1,4-α-D-glucanohydrolase, endoamylase), a protein known to hydrolyze starch, glycogen, and related polysaccharides by randomly cleaving the internal α-1,4-glucosidic linkages.[29] Microspheres of α-amylase were compared for their catalytic activity with those of the native protein.

To find the activity of α-amylase microspheres, the reduced sugar released during the reaction with starch as the substrate was measured. After a 3 min, it was found that when using native amylase as the enzyme 0.245 g of maltose was released, compared to the release of only 0.12 g when a suspension of microspheres was used. Hence, the activity of amylase microspheres after 3 min is only 50 % compared to native amylase. However, after 1 h 0.48 g of maltose was released when using the native amylase, and 0.34 g of maltose was detected when using the solution containing amylase microspheres. In this case the activity of amylase microspheres after 1 h is 70 % compared to the native amylase. The enzymatic activity of this solution was also measured at 10, 20, 30, 40 and 50 min. Figure 3 depicts graphs of released maltose versus reaction time for two samples of amylase microspheres prepared from two different concentrations of the protein. A linear relation of the maltose released versus time is obtained for the as-prepared microspheres. Zero-order kinetics is obtained, indicating that the concentration of the enzyme is limited, and hence, the product formation depends only on K_b (K_b is the rate at which the enzyme–substrate complex falls apart). This linear relationship is also reported for the release of maltose due to the activity of the same amount of native amylase on a similar amount of starch.[30] This comparison assumes that the measured microsphere suspension contains only amylase microspheres. However, perhaps not only the amylase microspheres are responsible for the high measured activity, but that some free amylase that did not undergo microsphere formation contributes as well. To assess the activity contributed solely by the microspheres, they were separated from the suspension by filtration. The determination of the enzymatic activity of the separated solution was done according to the same method. After 3 min, it was found that this solution yielded 0.0743 g of maltose, which is about 30 % relative to the native amylase. For comparison after 1 h, a concentration of 0.151 g of maltose was detected, which is about 31 % relative to the native amylase. This measured activity is due to the unreacted amylase that was left as the native enzyme after the sonication. These results indicate that the catalytic activity of the microsphere suspension is a sum of the activities of amylase microspheres and of native amylase. Assuming a complete separation between the microspheres and the rest of the solution, the results can be summarized as follows: a sample that produced 0.245 g maltose (after 3 min) yielded only 0.12 g maltose after sonication. Of the 0.12 g, 0.0743 g were produced as a result of the activity of the residues of unreacted native amylase; the remainder, 0.0457 g, is due to the enzymatic activity of the microspheres. These results show that 30 % of the amylase remained unreacted and 70 % were converted into microspheres. The enzymatic activity of these 70 % corresponds to

19% of that of the native enzyme. Therefore, if it is assumed that the comparison between the native and the microspherical protein should be made using equal amounts of enzyme, then the enzymatic activity of the microspheres amounts to 27% of that of the native amylase. The corresponding numbers after 1 h show again that only 31% of the enzyme remains unreacted. On the other hand, the catalytic activity of the microspheres is much higher and it reaches 56% of the native protein when equal masses are compared. This result indicates that the catalytic activity of the enzymatic microspheres is considerably slowed down relative to the native enzyme. The reduced activity is accounted for by arguing that some active sites of the enzyme might be buried inside the shell of the microspheres (the thickness is about 30 nm)[19] and are therefore inactive. However, it is possible that some soluble enzyme was locked in the center of the microsphere (in the organic media), and if this is the case, the activity will not increase. It is believed that if the enzyme is encapsulated inside the microsphere it will not penetrate through the shell of the microsphere, at least not within a few minutes. Hence, it will not react during the short measurement time. The rate at which the enzyme microspheres react is therefore a lower limit for its total activity. There is no question, however, that the microspheres are catalytically active, and that the microsphere formation process, unlike denaturation, does not destroy the active sites of the enzymes. However, it seems that approaching the active sites by the reactants becomes more difficult, and it causes the slow down of the reaction; part of the reactive sites cannot be reached at all.

In this study, a comparison of the enzymatic activities is always compared with a 3 and 60 min reaction time. This is done following the routine found in the literature.[29,31,32] Another possible explanation that might contribute or interpret the catalytic activity of the microspheres is as follows: it is possible that native amylase adsorbed on the surface of the microsphere causes the catalytic activity. To probe whether this hypothesis is a viable explanation, the sonicated solution was placed in a dialysis bag. The pore size of the dialysis membrane was 100 nm. The microspheres were repeatedly washed with distilled water to guarantee that all the native amylase escapes the bag into the pure water. After 48 h of rinsing, the enzymatic reaction was repeated and no reduction in the catalytic power was observed. This ascertains that the reaction progresses is through the active sites on the microspheres and is not due to the native enzyme.

The enzymatic activity was also measured for a less thermostable enzyme. α-Chymotrypsin microspheres were prepared by using the same sonochemical method as reported above, except that in this case an ice bath was used during the sonication. α-Chymotrypsin preferentially splits peptide bonds near hydrophobic residues. In addition, chymotrypsin catalyzes the hydrolysis of ester and amide bonds of aromatic amino acids, as well as proteins and peptides. The enzymatic activity of α-chymotrypsin microspheres was assayed by measuring the increase in the absorbance at 256 nm. This is the wavelength at which the hydrolysis products of benzoyl-L-tyrosine ethyl ester (BTEE) absorb. The enzymatic activity was compared with that of the native α-chymotrypsin. After 1 min the enzymatic activity of the α-chymotrypsin microspheres was 51% of that of the native protein, while over a longer reaction time (10 min) it reached 65% of the activity of the native protein. From those results it was concluded that using the sonochemical method for the preparation of enzyme microspheres is a very useful and easy method that does not destroy the enzymatic activity. In this research, it was demonstrated that the sonication leading to the modification into microspheres of two enzymes, amylase and α-chymotrypsin, is not a denaturation process. The PMs are catalytically active, but their reactivity is reduced as compared to the native protein.

Encapsulating a Drug in a Proteinaceous Microsphere

The creation of the microbubbles is a short process that lasts a few minutes. In Gedanken's laboratory the process was stopped after 3 min. It was demonstrated that if during this period a drug is found in the precursor mixture, it will be encapsulated in the PM. Tetracycline (TTCL) was successfully encapsulated in BSA microspheres.[33] TTCL is an antibiotic drug with a broad spectrum of activity, is a relatively safe drug that can be used by many routes of administration, and is widely used. The encapsulation was achieved in a one-step, 3 min, sonochemical process, starting with the native BSA protein and TTCL. The product was analyzed and characterized by scanning electron microscopy (SEM) and dynamic light scattering (DLS) measurements. The amount of TTCL loaded in the microspheres was also determined.

TTCL loaded in BSA microspheres was prepared by using the sonochemical method.[26] Mesitylene (97% Aldrich, 20 mL) was layered over of an aqueous BSA solution (albumin, bovine fraction v, σ, 30 mL, 5% w/v). A separation flask was used to separate the product from the mother solution. The separation was accomplished within a few minutes due to the lower density of the microspheres relative to water. We waited 24 h to ensure a complete phase separation. The preparation of TTCL-loaded microspheres was repeated by using a different concentration of the drug in the precursor solution. The amount of TTCL loaded in the microspheres was determined by subtracting the amount of the drug in the residual microsphere phase (the lower phase in the separation flask) from its total amount in the precursor solution. The sonochemistry did not destroy the TTCL, as evidenced by the very small changes in the TTCL concentration (less than 5%) that occur during sonication in the absence of BSA. No residue of TTCL was found in the excess mesitylene (the upper phase). The amount of TTCL loaded was assayed by using a Cary 100 spectrophotometer at 350 nm, and the actual values were calculated based on a calibration graph. The concentration of TTCL was computed in water in grams per 30 cm^{-3} of a liquid solution.[33]

The TTCL loading studies showed that the maximum TTCL loading capacity was found to be 65%. The percentage of the loaded drug in the BSA microspheres increased with the increase in the concentration of the TTCL in the original solution (Figure 4). However, this behavior changed

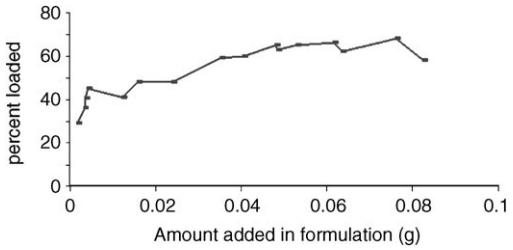

Figure 4. The amount of TTCL (%) that was encapsulated in BSA microspheres.

when the concentration of TTCL reached 3.6×10^{-3} M. At this concentration saturation is obtained, and the percentage of the drug in the microsphere does not grow with an increase of its concentration in the precursor solution. The increase in the amount of TTCL that was loaded in the microspheres can be explained by understanding the sonochemical method. The microspheres are formed by chemically cross-linking cysteine residues of the protein with an HO_2 radical formed around a micron-sized gas bubble or a nonaqueous droplet. The TTCL is hardly dissolved in the mesitylene. However it was found that TTCL partially dissolves in mesitylene after the sonochemical reaction. These results were found when applying the sonochemical reaction to a liquid solution that does not contain BSA. In this experiment, TTCL was found in the excess mesitylene. (The minimum ratio of the TTCL concentration in the residue aqueous phase and in the excess mesitylene phase was 22:1). The droplet of the solution trapped upon the collapse of the bubble encapsulates the mesitylene and the TTCL molecules. The higher the TTCL concentration in the solution, the higher the amount of TTCL loaded in the microspheres, until it reaches maximum. However, since the solubility of TTCL in mesitylene is limited, saturation is obtained when this limit is reached. The saturation reached at a certain percentage of entrapped TTCL is due to molecules of TTCL leaving the microspheres through the walls, and the equilibrium that is attained between leaving and entering the molecules.

An additional investigation was carried out to find whether the measured amount of tetracycline is due to molecules adsorbed on the outer surface of the sphere or due to the TTCL molecules encapsulated inside the microspheres. The first experiment involved heating (50 °C) the as-prepared solution in a separation flask for 5 h. TTCL that is adsorbed on the surface of the microspheres is known to dissolve in hot water. After a complete separation, the amount of TTCL in the residue phase (water) was measured. The average of a few experiments yielded 4% of TTCL adsorbed on the surface of the microspheres. The second experiment was carried out by measuring the absorbance of a sample of TTCL microspheres before and after washing with ethyl acetate/diethyl ether (6:4). The results yielded a value of 1–3% of TTCL adsorbed on the microsphere surface. The differences between the results of these two experiments can be explained by assuming that even during gentle heating (the first experiment), some microspheres can be destroyed. Nevertheless, these results indicate that most of the TTCL molecules are found inside the microspheres, and only a very small amount on its surface. The high capacity of the microspheres, produced by the sonochemical method, can be used in the future for antibiotic treatment.

The antimicrobial activity of the TTCL loaded in BSA microspheres was tested on two bacterial strains that are sensitive to TTCL. One strain, *Staphylococcus aureus*, represents the gram-positive bacteria and the other, *Escherichia coli*, represents the gram-negative bacteria. Each of the strains was spread on nutrient agar plates and 20 μL of the tested samples were put on seeded plates. Microspheres loaded with TTCL show an inhibition zone around both bacteria of 30 mm.[33] This inhibition zone was almost equal to the inhibition zones obtained by the TTCL that was freed from the microspheres by increasing the temperature or the zone of freshly prepared TTCL at the same concentration (30 μg). A TTCL disk that also contains 30 μg of the antibiotic was used in clinical diagnostics and showed the same inhibition zone. It seems that the TTCL trapped within the microsphere and released to the medium is equally active as the TTCL freed from the microspheres by heating. Both sonochemically treated TTCLs are active as antimicrobial agents to the same degree as TTCL that was not sonochemically treated.

In another study, PMs of BSA containing an anticancer drug (Taxol) were fabricated and characterized.[34] It was found that in the sonochemical reaction the drug did not decompose and was encapsulated inside the BSA microspheres. Anticancer activity of the PMs encapsulating the Taxol was tested on multiple myelonoma cells. That means that when compared to the tetracycline study,[33] the drug cannot only be encapsulated in the microsphere, but can also be released and kill the desired cells. Taxol has been approved by the FDA for the treatment of ovarian cancer, breast cancer, nonsmall cell lung carcinomas, and Kaposi's sarcoma.

The three starting materials that were used for the preparation of PMs containing the anticancer drug were: 1) A Taxol (Paclitaxel) injection (6 mg mL^{-1}, Mead Johnson, Oncology Products); 2) a 5% w/v aqueous solution of BSA (96–99% Aldrich); and 3) mesytilene (98% Fluka). The amount of Taxol in all reactions was varied from 5–300 μL. The volumes of the 5% (w/v) BSA solution and of mesytilene were kept constant (30 and 20 mL, respectively). The Taxol was added to mesitylene and the solution was layered over a BSA solution. The volumes of the 5% (w/v) BSA solution and of mesytilene were kept constant (30 and 20 mL, respectively). The Taxol was added to mesitylene and the solution was layered over a BSA solution. The amount of

Taxol loaded into the microspheres was determined by using reversed-phase, high-performance liquid chromatography (RP-HPLC), and the actual values were calculated from a calibration graph. HPLC analyses were carried out using a LiChrospher 100 RP-18 column (250×4.6 mm i.d.; 5 μm) under isocratic conditions with acetonitrile/water (55:45, v/v) at a flow rate of 1 mL min^{-1}. Spectral data from the UV detector were collected at 227 nm. The calibration graph was constructed by dissolving known amounts of Taxol in methanol. The anticancer activity of the BSA microspheres containing Taxol was tested on multiple myeloma cells (cancer cells). Different amounts of microspheres containing Taxol (5–30 μL) were added to suspensions of these cells. After a 24 h incubation at 37 °C, the cells were analyzed by using visible-light microscopy and a fluorescence-activated cell sorter (FACS).

A wide distribution of the BSA–Taxol microbubbles was measured ranging between 300 and 2500 nm, falling more sharply between 800 and 1500 nm.[34] Different concentrations of the drug in the precursor solution were used in order to synthesize PMs containing various amounts of Taxol. When the amount of Taxol dissolved in the organic solvent was in the range of 100–300 μL, no PMs were produced. Taxol-loaded microspheres were prepared and separated successfully only when the volume of Taxol added to the mesytilene was in the range of 5–100 μL. The concentration of Taxol encapsulated inside the microspheres or adsorbed on the outer surface of the microsphere was determined by subtracting the concentration of the drug in the residual microsphere phase (the upper phase in the separation flask) from its initial concentration in the precursor solution. No residue of Taxol was found in the aqueous phase.

The results of the Taxol loading are summarized in Figure 5. This graph shows the relationship between the initial concentration of Taxol in solution and the amount of the drug that was encapsulated in the microspheres. The percentage of the encapsulated drug in the BSA microspheres increased with the increase in the concentration of Taxol in the initial solution. The maximum loading capacity of Taxol was found to be above 90 %.

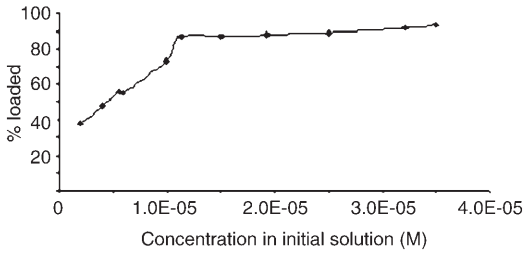

Figure 5. The amount of Taxol (%) encapsulated in BSA microspheres.

The anticancer activity of the BSA microspheres loaded with Taxol was tested on multiple myeloma (cancer cells). Different amounts of microspheres containing Taxol (5–30 μL) were added to suspensions of these cells. After a 24 h incubation at 37 °C, the samples were analyzed by using visible-light microscopy and an FACS. The range of Taxol concentration in the microspheres that were tested was between 8×10^{-7} M and 3.49×10^{-5} M. The Taxol was freed from the microspheres due to the presence of proteases in the medium. The cancer cells that were treated with Taxol-loaded BSA microspheres were first tested under visible-light microscopy, and the number of dead cells was counted by using trypan-blue staining. When the Taxol concentration in the BSA microspheres was in the 1.5×10^{-5}–3.49×10^{-5} M range, a total killing of the cancer cells was achieved. All the results in Table 1 were measured when the concentration of the drug inside the microsphere was 1.3×10^{-6} M. It can be seen that the number of dead cells measured after the microsphere treatment was almost equal to the number of dead cells counted after using the same concentration of freshly prepared Taxol. The same behavior (equal killing by microspheres and pristine Taxol) was observed when the concentration of the drug inside the microsphere was between 8×10^{-7} M to 1.5×10^{-5} M. It is important to point out that in all cases a higher Taxol concentration in the BSA microspheres always led to a higher percentage of dead cells in the tissue culture.

Table 1. Number of dead cancer cells observed after treatment with different amounts of Taxol loaded in BSA microspheres.

Type of treatment	% of dead cells
5 μL of Taxol-loaded microspheres (c Taxol inside $=1.3\times10^{-6}$ M)	27
10 μL of Taxol-loaded microspheres (c Taxol inside $=1.3\times10^{-6}$ M)	52
20 μL of Taxol-loaded microspheres (c Taxol inside $=1.3\times10^{-6}$ M)	78
5 μL of Taxol ($c=1.3*10^{-6}$ M)	21

Taxol inhibits cell division at the G_2–M interface, so that after treatment with the drug one expects to see an increase in the number of cells in the G_2–M phase and in the apoptotic cell population when the increase in the G_2–M is more evident than the increase in the number of dead cells. The purpose of the second examination of the anticancer investigation was to test whether Taxol loaded in the microsphere acts in the same manner as the original native Taxol. Therefore, after the cancer cells were treated with microspheres, they were examined by an FACS, which performs a cell-cycle distribution and counts the number of cells in each phase of the cell cycle. The results are summarized in Table 2. It can be shown that after treatment with microspheres there is an increase in the apoptotic cells, which is greater than the increase in the G_2–M phase of the cell cycle.

An additional step was carried out to determine whether Taxol in combination with mesytilene, or only mesytilene, causes the death of cancer cells. In this experiment three samples of Taxol-loaded microspheres with different drug

Table 2. Number of cells in the G_2–M phase and in the apoptotic phase observed after treatment with different amounts of Taxol loaded in BSA microspheres.

Type of cells	Cells in the G_2–M phase [%]	Dead cells (apoptosis) [%]
cancer cells before treatment	22	6
cancer cells after treatment with original Taxol ($c = 5 \times 10^{-6}$ M)	45	23
cancer cells after treatment with microspheres (c Taxol inside $= 5 \times 10^{-6}$ M)	15	38

concentrations were tested. It was found that the increase in the amount of Taxol in the microspheres leads to an increase in the number of cells in the G_2–M and apoptotic phases. This experiment shows clearly that the Taxol has an additional killing effect beyond the mesytilene activity.

Makino et al. were interested in the release of a drug from the PM and their model compound was Sudan III, which was dissolved in chloroform and was loaded into microcapsules with membranes composed of BSA.[35] The permeability of Sudan III through the microcapsule membrane to chloroform was examined as a function of a Sudan III concentration in the microcapsule core, as well as the temperature. The release of Sudan III from microcapsules to a sodium lauryl sulfate (SLS) solution was studied. The concentration of Sudan III was measured spectrophotometrically at 500 nm. In distilled water, the released amount increases in the initial 100 h, and then remains at an almost constant value. In a 0.5% (w/v) SLS solution, Sudan III is released slowly between 24 and 150 h, after a faster release observed in the initial 24 h. After 150 h, the release rate increases until 200 h, and then becomes almost zero. In a 1% (w/v) SLS solution, the release rate is low in the initial 60 h, becoming high between 60 and 80 h, and then almost zero after 100 h.

The membrane permeability of Sudan III was evaluated at 25, 30, and 37 °C in chloroform. A lag phase was observed in the time course of the permeation, the length of which was temperature-dependent. It was found that the length of the lag phase was explained by the activation energy. The Arrhenius plot of the reciprocal of the lag time suggests that the existence of the lag phase is associated with activation energy, which was was evaluated to be 60 kJ mol^{-1}.

Controlling the Size of Proteinaceous Microspheres, Yield of Microsphere Formation, and Coating Its Surface

The question of whether smaller PM can be obtained was addressed by Makino and co-workers.[36] They have checked the effect of a few variables on the yield of the BSA microspheres. In addition, they also monitored the effect of a few parameters on the size of the microspheres. They varied the following parameters: 1) effects of BSA concentration; 2) effects of toluene volume fraction in the mixture of toluene and BSA solution; 3) effects of acoustic frequency and irradiation time period; and 4) effects of the kind of the core (toluene, chloroform, peanut oil, or soybean oil) materials. They studied the effect of all four parameters on the yield of PM formation. In addition, they investigated the effect of third and fourth points on the size distribution.

They found that as the concentration of bovine serum albumin increases from 0.005 to 0.02% (w/v), the micro encapsulation yield increases. These measurements were conducted by adding toluene (1 mL) to an aqueous solution of BSA (10 mL) with various concentrations ranging from 0.001 to 5% (w/w). After the microencapsulation process, the remaining volume of oil not encapsulated in the BSA microcapsules, was measured, after which the yield of microcapsules was calculated. They reached the maximum yield of 85% at a (w/v) concentration of 1%. In fact from 0.02–1% only small changes in the yield were observed. At concentrations below 0.02% (w/v), drastic changes in the microsphere formation yield were measured. They interpreted the results as originating from the diluted solution, in which the frequency of the collision of BSA molecules is low and the density of the microcapsule membrane seems to be low, which in turn decreases the microsphere formation yield.

The influence of the toluene volume fraction on the microsphere formation yield becomes remarkable only above a value of 0.4; up to this value it is constant at a level of $\approx$80% yield. The microsphere formation yield decreases when the volume fraction of toluene becomes higher than 0.4. In addition, when the volume fraction of toluene is over 0.8, the phase inversion from o/w emulsion to w/o emulsion is clearly observed.

In Figure 6, the microsphere formation yield was plotted as a function of irradiation period and acoustic frequency.

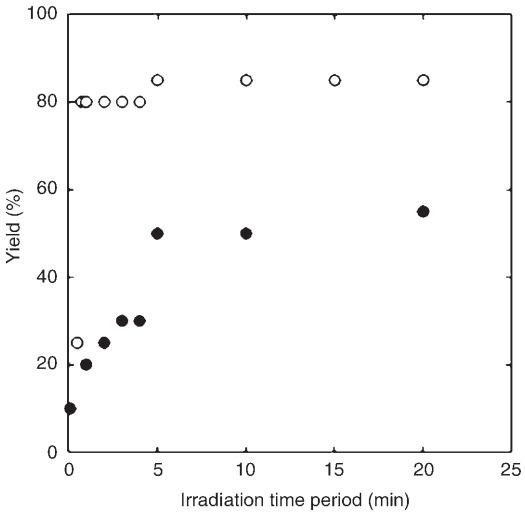

Figure 6. Effects of acoustic frequency and irradiation time period upon microencapsulation yield. Acoustic frequency was 28 ○ and 45 kHz ●.

The microsphere formation yield was higher at 28 than at 45 kHz, and no microcapsule was obtained at 100 kHz. As the irradiation time period increases, the microencapsulation yield increases at 45 kHz, but then remains almost constant after 5 min. Also, the dependence of the microencapsulation yield upon the irradiation time period was more clearly observed at 45 kHz than at 28 kHz, since at 28 kHz, the microencapsulation yield reaches almost 80% within 30 s.

Size dependence: Microcapsules with narrower size distributions have been obtained at 45 rather than at 28 kHz.[36] In addition, the volume-averaged diameter of the microcapsules is larger at 28 than at 45 kHz. The diameter of each kind microcapsule is about 3.81 and 2.66 μm, respectively. The authors also studied the influence of the organic liquid on the size distribution of the microspheres.[36] Using chloroform as the organic liquid resulted in capsules with an average diameter of 5.15 and 3.63 μm at 28 and 45 kHz, respectively. BSA microcapsules containing chloroform show a wider size distribution and a larger average size than BSA microcapsules containing toluene. Toluene is less miscible with water than chloroform; hence, the interface between toluene and water is much clearer than that between chloroform and water. Such a difference of solubility of two organic solvents to water may make the size distribution of microcapsules containing each organic solvent different. The size distributions of BSA microcapsules containing soybean oil and peanut oil were narrower than those obtained for toluene and chloroform. The volume-averaged diameters are 1.48 and 1.67 μm, respectively. The authors concluded[36] that smaller microcapsules are considered to be obtained when the encapsulated organic solvent has a higher viscosity. They did not provide an explanation for this observation.

Proteinaceous bubbles of 185 nm average diameter were synthesized by a sonochemical treatment of bovine serum albumin (BSA) in an aqueous solution.[37] In parallel, a solution of nanoparticles of TiO_2 was also made by ultrasonic irradiation. To study the macroscopic flow behavior associated with the changes in the state of the microparticles, a flow test of these solutions in microchannels was done. The authors measured by a light scattering method the size distributions of the proteinaceous bubbles in solution before and after the flow test. The authors noted that the PM they obtained were unusually small, about an order of magnitude smaller than that in all the other reports. The flow results show that the air-filled proteinaceous bubbles in solution adjust their size to reduce the shear stress encountered in the flow through the microchannel.

To reduce the microbubbles size to the nanometer range, Avivi has investigated the influence of adding a surfactant to the protein solution.[38] Two proteins were examined, BSA and α-amylase. The surfactants used in these experiments were SDS (sodium dodecyl sulphate), CTAB (cetyltrimethyl ammonium bromide), Oleic acid, Tween 40, and Tween 80. The concentration of the BSA was 3% w/v, and that of the α-amylase 0.0025% w/v. For all surfactants, a bimodal distribution was obtained. The distribution consisted of a major part of micron-sized microcapsules and only a small percentage of proteinaceous nanobubbles. However, the addition of Tween 80 had a dramatic effect on increasing the percentages of the nanospheres, and with larger amounts of this surfactant a situation was reached in which only nanobubbles are obtained. The same effect was obtained for the two proteins. For example, when 4 mL of the Tween 80 were used, all the amylase nanospheres were obtained in the 100–500 nm range; however, when 0.5 mL of the Tween 80 was added, 28% of the spheres were in the range of 600–1200 nm and 74% in the 60–500 nm range. In general, smaller nanospheres are obtained for amylase than for the BSA. Whether it is due to the smaller concentration or not is still under study.

The use of a surfactant in stabilizing polymeric microspheres is well known.[39,40] In a spherical structure the pressure inside the sphere is directly proportional to its surface tension and inversely proportional to its radius. The surfactant, which is composed of hydrophobic and hydrophilic ends, is organized around the sphere in a very specific way that ultimately reduces the surface tension, and at the same time, its radius.

Coating the PM surface: Magnetic PM,[43] containing nanophased iron oxide, have recently been fabricated by combining the previous sonochemical synthesis of nanostructured iron oxide[41,42] with Suslick's sonochemical synthesis of proteinaceous microspheres.[1,18–20] Decane and iron pentacarbonyl $Fe(CO)_5$ (7.43×10^{-4} M) were layered over a 5% w/v BSA solution. In parallel in a second experiment, the same procedure was performed with an aqueous solution of iron acetate, $Fe(CH_3CO_2)_2$ 95% (sigma)[2] (7.66×10^{-3} M).[43] To determine the amount and location of the Fe^{3+} ions, two experiments were conducted. First, the Fe^{3+} on the PM surface was determined. A second experiment determining the total amount of Fe^{3+} was performed after destroying the microspheres. The destruction of the microspheres happened when they were gently heated while mixing them with a magnetic stirrer for a few minutes, leading to a yellow homogeneous solution. After that the conventional method with thiosulfate and potassium iodide was used for the quantitative analysis of Fe^{3+}. Both determinations were performed for BSA microspheres with iron pentacarbonyl and for BSA microspheres with iron acetate. The concentration of Fe^{3+} ions on the surface was 7–9% w/w for both samples. The full weight of the microspheres (100%) included the weight of the solvent encapsulated in the core of the sphere. Following the above-mentioned process for the destruction of the microspheres, the total concentration of Fe^{3+} ions was found to be 39–42%. This implies that the major parts of the Fe^{3+} ions are trapped inside the spheres. The higher concentration of the iron oxide in the sphere's volume in the iron acetate reaction can be rationalized. The Fe^{3+} ions trapped inside the sphere are unaffected by the sonochemical process, and they are determined only by the original concentration of the iron acetate solution. The number of Fe^{3+} ions inside the sphere and on the surface was calculat-

ed. A monolayer coverage of the surface was assumed, and the area occupied by one Fe_2O_3 molecule as 20 $Å^2$. These calculations led to a ratio of 1.75:1 for the surface/inside Fe^{3+} ions. The measured ratio is 0.3:1, which indicates that only one-sixth of the outer surface is covered by Fe_2O_3 molecules. The size of the iron oxide nanoparticles was obtained from TEM and SEM measurements. The major part of the particles are in the 10–20 nm range; however, some aggregation is also observed and iron oxide particles of up to 200 nm can be identified. Detailed magnetic measurements of the magnetic PM were carried out. They include mangnetization loops at various temperatures, isothermal magnetization curves at various temperatures, and variation of the magnetic moment with temperature under a low (38 Oe) and high (10 kOe) magnetic fields. Based on the magnetic data and Mössbauer spectroscopy measurements, the following conclusions were reached

1) Preparing the PM with FeAc (acetates) produces a higher percentage of large particles than when preparing them with $Fe(CO)_5$.
2) The washing procedure (with HCl) affects the FeAc sample much more than the $Fe(CO)_5$, in the sense that the small particles are predominantly washed away (not so in $Fe(CO)_5$).
3) A rough estimate of the spread in particle sizes in all samples can be obtained from the 300 K Mössbauer spectra, when compared with known size of Fe_2O_3 small particle spectra. The diameter of most particles is less than 20 nm.

Selective targeting of protein microspheres to tumors, a natural extension after the encapsulation of a drug in the PM, was demonstrated. Recently, Suslick and co-workers[44] reported on a noncovalent, electrostatic layer-by-layer (LBL) modification that successfully targets protein microspheres to the integrin receptors that are over expressed in several tumor types. The protein microspheres are core-shell vesicles with a vegetable oil core and a BSA shell that is made up of plates of cross-linked protein subunits, which tile over the oil core like armadillo scales.[44] These core-shell microspheres are highly charged due to the numerous ionizable groups present in the BSA shell. Under physiological conditions, BSA typically has 185 counterions resulting from both acidic and basic surface residues, with a net charge of −17 at pH 7.[44] For a typical 2 μm microsphere, there are $\approx 10^6$ BSA molecules per shell. Thus, the protein microspheres are sufficiently charged for the electrostatic adhesion of polyelectrolytes onto their surface. Suslick has found that these negatively charged vesicles are excellent templates for LBL electrostatic adhesion. It was demonstrated[44] that PMs can be selectively targeted to human tumor cells by using an LBL approach to modify their surface with integrin-receptor-specific peptide ligands. Integrin receptors are overexpressed in several tumor types, and the RGD tripeptide motif has been used as a label for these tumor cells and their vasculature. Suslick and co-workers[44] synthesized three different peptides with an RGD motif embedded at the ends or in the middle of a highly positively charged, polylysine sequence: at the amino terminus, RGDKKKKKK; in the middle, KKKKRGDKKK; and at the carboxy terminus, KKKKKKKRGD.[45] The positively charged lysine residues electrostatically secure the RGD motif to the surface of the microspheres. The purified peptides are then used in the LBL electrostatic adhesion to decorate the surface of the protein microspheres. The success of the adhesion was determined by measuring the ζ potential (i.e., net particle charge) of the microspheres before and after adhesion of the peptides. The ζ potential of the microspheres varied from −54 mV before modification to +22 mV after peptide adhesion occurred. In a second approach taken by Suslick and co-workers,[43] the microspheres were exposed first to the polycationic RGD-containing peptides to reverse their surface charge, and then to silica colloids (≈100 nm), which are negatively charged at pH 7.4 and do not adhere to native (i.e., negatively charged) BSA microspheres. They determined the efficacy of the RGD-modified microspheres in tumor targeting by using HT29 tumor cells, which are human colon tumor cells known to overexpress integrin receptors, in vitro.

Microspheres Made of Proteins that Do Not Contain Cysteine

The importance of cysteine and the formation of S–S bonds in the creation of the PM was emphasized by Suslick from the early stages of this field.[1] To probe whether the sonochemical microsphere formation process is more general and can be applied to proteins that do not contain a thiol, an attempt was made employing this method to streptavidin. Streptavidin is a protein very similar to avidin, but is nonglycosylated and devoid of any sulphur residues. Avivi has extended[46] the sonochemical method to this non-sulphur-containing protein, strepavidin and demonstrated the formation of PMs. The microspheres are stable for many hours at room temperature and for at least one month at 4 °C. No microspheres were obtained when the pH was kept at 7. However, when the pH was lowered to 6.0 by adding concentrated HCl, microspheres were formed. It is very important to note that adding a concentrated acid did not create any local denaturation. To prove that the pH is important in the formation of the PMs, they also conducted the reaction under mild conditions using a buffer (pH 6) and obtained the same microspheres. In Figure 7, a SEM image of the streptavidin microspheres that were fabricated on the sonochemical reaction is presented. The morphology of the microspheres made of sterptavidin is very similar to that obtained in previous studies. The size distribution of the microspheres was measured by dynamic light scattering and the average size was found to be 5 μ.

The role of the acidic medium in a sonochemical mechanism is explained as follows. Ultrasonic irradiation of liquids is known to produce both emulsification[19] and cavita-

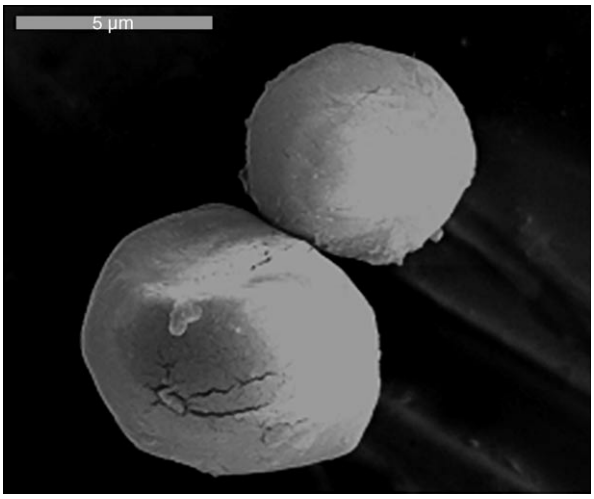

Figure 7. Scanning electron micrograph of streptavidin microspheres (bar = 5 µm). The microspheres were prepared for SEM by secondary cross-linking with glutaraldehyde and by coating with Au.

tion.[1,15] Emulsification alone, however, is insufficient to form long-lived microspheres. It was found that the microspheres are held together by protein cross-linking through disulphide linkages from cysteine oxidation.[1,18,19] However, it is evident that this is not the mechanism for the formation of strepravidin microspheres. According to the proposed explanation, hydrophobic or thermal denaturation of the protein after the initial ultrasonic emulsification assists in microsphere formation. According to Lins and Brasseur,[47] the hydrophobic effect drives the molecules towards a more condensed structure by decreasing the unfavorable contacts between the hydrophobic residues and water molecules. A minor contribution is provided by the lowering of the pH, which helps to neutralize the basic COO^- edges, thus creating a more favorable hydrophobic environment. To check whether this hypothesis is correct, a polyglutamic acid (σ) protein was sonicated. This protein carries only carboxyl groups on the side chain. The concentration of the solution was 5% w/v, with all the other sonochemical parameters remaining unchanged. Microspheres of the polyglutamic acid were formed only at a pH lower than 4.5. This pH is lower than the pK_a of the side group of this polymer (the pK_a of the side chain carboxyls of aspartic and glutamic acids is 4–4.8). Thus it can be concluded that hydrophobic interactions, which become more dominant in an acidic medium, are responsible for the production of the microspheres in a polyglutamic acid, as well as in streptavidin. Such hydrophobic interactions are strong enough to produce microspheres that are stable for at least one month.

The ability of streptavidin microspheres to bind biotin was also checked, and compared to commercial native streptavidin. It was found that streptavidin microspheres bind about 50% of the amount of biotin bound to the native protein. It was also found that the biological activity of proteinaceous microspheres is reduced by 30–50%, as compared with the native protein.

Suslick and co-workers have prepared[48] a new class of protein core-shell microspheres made with polyglutamic acid, the size of which is sufficiently small to permit extravasation (i.e., escape) from the blood pool, particularly in regions with leaky vasculature, for example, tumors. In contrast to previous core-shell protein microspheres (generally made from serum albumin), these sodium polyglutamate (SPG) microspheres are not held together by covalent cross-links, and yet they are extremely stable. A 5 wt% solution of sodium poly(α,L-glutamate) (SPG) was layered with vegetable oil and then sonicated using a 2 mm diameter ultrasonic tip (20 kHz, 50 $W cm^{-2}$, 3 min), which produces spheres that are less than one micron in diameter. These microspheres are core-shell, as shown in the cross-sectional TEM image. The thermal stability was tested, and the SPG microspheres were stable for more than an hour even at 60 °C.

The intermolecular interactions that might be responsible for holding the SPG microspheres together include hydrogen bonding, van der Waals, hydrophobic, and electrostatic interactions, all of which can be effected by changes in pH and ionic strength. More specifically, the authors[48] believe that the dominant interaction between the polymer chains are a network of hydrogen bonds or ion pairs: $[RCO2^{-}\cdots M^{+}\cdots{}^{-}O2CR]$ in which $M^+ = H^+$ or Na^+.

Applications of the Proteinaceous Microspheres

Some of the applications of PMs have already been mentioned and discussed throughout this review, in particular in the chapter dealing with the encapsulation of drugs inside the PM and the release of these drugs. It is, however, worth mentioning some other applications. Suslick[49] has fabricated PMs filled with nitroxides dissolved in an organic liquid by using high intensity ultrasound methods; the PMs were used to measure oxygen concentrations in living biological systems. The microspheres have an average size of 2.5 µm, and the proteinaceous shell is permeable to oxygen. Encapsulation of the nitroxides into the microsphere greatly increased the sensitivity of the EPR-signal line width to oxygen because of the higher solubility of oxygen in organic solvents. The encapsulation also protected the nitroxide from bioreduction. No decrease in the intensity of the EPR signal was observed over a 70 min period after the intravenous injection of the microspheres into a mouse. Measurement of the changes in oxygen concentration in vivo by means of the restriction of blood flow, anesthesia, and change of oxygen content in the respired gas, were made using these microspheres.

Suslick and co-workers have used PMs for increasing the signal-to-noise ratio (SNR) of fluorine magnetic resonance imaging and enabling new applications.[50] They have developed a novel class of agents based on the protein encapsulation of fluorocarbons. Microspheres formed by high-intensity ultrasound have a gaussian size distribution with an average diameter of 2.5 µm. As with conventional emulsions,

these microspheres target the reticuloendothelial system. However, the sonochemically produced microspheres, which leads to a high encapsulation efficiency, show increases in the SNR of up to 300% compared to commercially available emulsions. They have demonstrated an increase in the circulation lifetime of the microspheres within the bloodstream by more than 80-fold with a chemical modification of the outer surface of the microsphere. Finally, by encapsulating mixtures of fluorocarbons that undergo solid/liquid phase transitions, they have mapped the temperature in the reticuloendothelial system, with signal changes of approximately 20-fold over a 5°C range.

They proposed that PMs might have a wide range of biomedical applications, including their use as echo contrast agents for sonography, magnetic resonance imaging contrast enhancement, and oxygen or drug delivery

More recently Lee et al. characterized and demonstrated[51] a new class of optical contrast agents suitable for reflection- or scattering-based optical imaging techniques, namely, OCT (optical coherence tomography), but that also includes light and reflectance confocal microscopy. These agents are biocompatible, are suitable for in vivo use, and produce an enhanced backscatter that is detectable in highly scattering tissue. These agents may be tailored to adhere to specific molecules, cells, or tissue types, and thus provide additional selectivity that can enhance the utility of OCT as an emerging diagnostic technique. OCT is capable of cellular-resolution imaging and may ultimately have a role in the early diagnosis of human malignancies. The authors have engineered optical contrast agents that are microspheres 0.2–15 μm in diameter with an approximately 50 nm-thick protein shell. The microspheres are designed to incorporate in their shells, and encapsulate in their cores, a wide range of nanoparticles and materials that alter the local optical properties of tissue. The protein shell was also functionalized to target the agents to specific regions of interest. The authors have sonicated a 5% weight per volume solution of BSA and a solution containing the material to be incorporated into the shell or encapsulated in the core. They have measured the optical properties of gold-, melanin-, and carbon-shelled contrast agents and demonstrated the enhancement of optical coherence tomography imaging after the intravenous injection of such an agent into a mouse.

Miscellaneous

In this chapter we plan to present and discuss some publications related to PMs, but that do not fit the sub-sections of the current review.

Shiomi and co-workers[52] have fabricated hollow spherical particles with protein/silica-hybrid shell structures. The synthesis was based on a combination of the catalytic activity of the protein and sonochemical treatment. The reaction started with lysozyme powder derived from egg whites, which is put into a 0.05 M glycine buffer at given concentrations. The lysozyme solution was brought to pH 9 by the addition of 5 N NaOH, after which TEOS (tetraethoxysilane, 1 mL) was added. The mixture was immediately stirred or sonicated for 15 min. The resultant solutions were dispensed onto a polystyrene plate and dried at 60°C for 24 h, after which a white powder was obtained. The granular spherical particles obtained at the end of the reaction have a diameter of 250–1000 nm. No spherical particles were observed without lysozyme in the reacting solution, suggesting that the biomimetic patterning of silica can be catalyzed by lysozyme. When sonication treatment was applied to the lysozyme–TEOS mixture, hollow spherical particles were observed.

In short, the authors demonstrated that the morphologies of the particles can be controlled by altering reaction conditions (stirring or sonication) or by changing lysozyme concentrations. Furthermore, the method needs no process to remove the template, which is inevitable in other protocols used to obtain hollow silica particles. The authors claim that the method for the formation of inorganic–organic hybrids induced by biopolymers, as described herein, sheds light on the controlled formation of silica structures and goes some way to the creation of advanced materials.

Another group that have sonicated a range of structurally diverse proteins have observed the formation of aggregates that have similarities to amyloid aggregates.[53] The formation of amyloid is associated with, and has been implicated in, causing of a wide range of protein conformational disorders including Alzheimer's disease, Huntington's disease, Parkinson's disease, and prion diseases. The aggregates cause large enhancements in the fluorescence of the dye thioflavin T. Ultrastructural analysis by electron microscopy reveals a range of morphologies for the sonication-induced aggregates, including fibrils with diameters of 5–20 nm. The addition of preformed aggregates to unsonicated protein solutions results in the accelerated and enhanced formation of additional aggregates upon heating. The dye-binding and structural characteristics, as well as the ability of the sonication-induced aggregates to seed the formation of new aggregates, are all similar to the properties of amyloid.

High-intensity ultrasonic irradiation of aqueous solutions of $Ca(H_2PO_4)_2$ and $Ca(OH)_2$ in the presence of BSA has led to the formation of calcium phosphate/albumin colloidal particles.[54] The effect of the concentration of BSA (2–5 $g\,L^{-1}$) properties of the colloidal particles was studied at constant temperature. The formation mechanism of CaP/BSA colloidal particles seems to be similar to the mechanism of the sonochemical formation of albumin and haemoglobin microspheres .[1] According to this mechanism, the nanospheres are held together by disulfide bonds between protein cysteine residues; HO_2 radicals, sonochemically produced by acoustic cavitation, act as the cross-linking agent. This chemical cross-linking is responsible for the formation of the netlike morphology of CaP/BSA colloidal particles. The particle size was dependent on the concentration of the BSA. For 4 $g\,L^{-1}$ of BSA, the average particle size was 87 nm and the distribution width was 98 nm. The average ζ potential of the CaP/BSA particles was −25.5 mV, and it was only slightly affected by the concentration of BSA.

Finally, Zhong and associates studied the effects of ultrasound and additives on the function and structure of trypsin.[55] They tried to investigate the effects of ultrasound power and duration of irradiation on the function and structure of trypsin, and the reason for protein denaturation when it was irradiated by 20 kHz ultrasound. The damage to the molecular structure of trypsin was detected through a combination of high-performance liquid chromatography and electrospray ionization mass spectrometry (HPLC-ESI-MS). The results showed that the activity of trypsin decreased with increasing ultrasound power from 100 to 500 W, or with extended the irradiation time from 1 to 20 min. This effect could be enhanced by aerating the solution for 10 min at 300 W. Fragments of trypsin were detected in the treatment (300 W, 10 min) by HPLC-ESI-MS. The additives Tween 80 and mannitol could protect trypsin against the inactivation caused by ultrasound. The reason for this inactivation was partly from the alteration of the molecular conformation and partly from the modification or damage to the trypsin's molecular structure.

[1] K. S. Suslick, M. W. Grinstaff, *J. Am. Chem. Soc.* **1990**, *112*, 7807, and references therein.
[2] T. J. Mason, *Sonochemistry*, Royal Society of Chemistry, London, **1990**.
[3] "Sonochemistry and Other Novel Methods Developed for the Synthesis of Nanoparticles": A. Gedanken, Y. Mastai, in *The Chemistry of Nanomaterials, Vol. 1* (Eds.: C. N. R. Rao, A. Muller, A. K. Cheetham), Wiley-VCH, Weinheim, **2004**, pp. 113–169.
[4] A. Gedanken, *Ultrason. Sonochem.* **2004**, *11*, 47.
[5] K. S. Suslick, G. J. Proce, *Annu. Rev. Mater. Sci.* **1999**, *29*, 295.
[6] Y. G. Adewuyi, *Ind. Eng. Chem. Res.* **2001**, *40*, 4681.
[7] L. H. Thompson, L. K. Doraiswamy, *Ind. Eng. Chem. Res.* **1999**, *38*, 1215.
[8] a) R. Hiller, S. J. Putterman, B. P. Barber, *Phys. Rev. Lett.* **1992**, *69*, 1182; b) B. P. Barber, S. J. Putterman, *Nature* **1991**, *352*, 414.
[9] K. S. Suslick, S. B. Choe, A. A. Cichowlas, M. W. Grinstaff, M. W. *Nature* **1991**, *353*, 414.
[10] K. S. Suslick, D. A. Hammerton, R. E. Cline, *J. Am. Chem. Soc.* **1986**, *108*, 5641.
[11] C. D. Dick, S. B. Feinstein, *Pract. Cardiol.* **1988**, *14*, 69.
[12] S. B. Feinstein, M. W. Keller, C. D. Dick, *J. Am. Coll. Cardiol.* **1987**, *9*, 111A.
[13] M. W. Keller, S. B. Feinstein, R. A. Briller, *J. Ultrasound Med.* **1986**, *5*, 493.
[14] S. B. Feinstein, F. J. Tencate, W. Zwehl, K. Ong, G. Maurer, C. Tei, P. M. Shah, S. Meerbaum, E. Corday, *J. Am. Coll. Cardiol.* **1984**, *3*, 14.
[15] K. S. Suslick, *Science* **1990**, *247*, 1439.
[16] M. Del Duca, E. Jeager, M. O. Davis, F. Hovarka, *J. Acoust. Soc. Am.* **1958**, *30*, 301.
[17] B. Lippitt, J. M. McCord, I. Fridovich, *J. Biol. Chem.* **1972**, *247*, 4688.
[18] M. W. Grinstaff, K. S. Suslick, *Proc. Natl. Acad. Sci. USA* **1991**, *88*, 7708.
[19] K. S. Suslick, M. W. Grinstaff, K. J. Kolbeck, M. Wong, *Ultrason. Sonochem.* **1994**, *1*, S65.
[20] M. Wong, K. S. Suslcik, *Mater. Res. Soc. Symp. Proc.* **1995**, *372*, 1195.
[21] A. Hyashi, T. Suzuki, M. Shin, *Biochim. Biophys. Acta* **1973**, *310*, 309.
[22] K. Imai, H. Morimoto, M. Kotani, H. Watari, W. Hirata, M. Kuroda, *Biochim. Biophys. Acta* **1970**, *200*, 189.
[23] S. Avivi, A. Gedanken, *Ultrason. Sonochem.* **2005**, *12*, 405.
[24] S. Avivi, A. Gedanken, *Ultrason. Sonochem.* **2007**, *14*, 1.
[25] N. M. Green, *Adv. Protein Chem.* **1975**, *29*, 85.
[26] N. M. Green, *Biochem. J.* **1965**, *94*, C23.
[27] R. Hawkers, *Anal. Biochem.* **1982**, *123*, 143.
[28] G. Gitlin, A. E. Bayer, M. Wilchek, *Biochem. J.* **1990**, *269*, 527.
[29] S. Tei-Fu, L. Fu-Pang, C. Su-Chin, C. Hsing-Chen, *Bot. Bull. Acad. Sin.* **1995**, *36*, 195.
[30] R. A. Kaufman, N. W. Tietz, *Clin. Chem.* **1980**, *26*, 846.
[31] P. Bernfeld, *Adv. Enzymol. Relat. Areas Mol. Biol.* **1951**, *12*, 379.
[32] P. Bernfeld, *Methods Enzymol.* **1955**, *1*, 149.
[33] S. Avivi, Y. Nitzan, R. Dror, A. Gedanken, *J. Am. Chem. Soc.* **2003**, *125*, 15712.
[34] O. Grinberg, M. Hayun, B. Sredni, A. Gedanken, *Ultrason. Sonochem.* **2007**, *14*, 661.
[35] K. Makino, T. Mizorogi, S. Ando, T. Tsukamoto, H. Ohshima, *Colloids Surf. B* **2002**, *23*, 59.
[36] K. Makino, T. Mizorogi, S. Ando, T. Tsukamoto, H. Ohshima, *Colloids Surf. B* **2001**, *22*, 251.
[37] J. Y. Jung, K. T. Byun, H. Y. Kwak, *Microfluid. Nanofluid.* **2005**, *1*, 177.
[38] S. Avivi, A. Gedanken, unpublished results.
[39] C. Wu, *Macromolecules* **1994**, *27*, 298.
[40] C. Wu, *Macromolecules* **1994**, *27*, 7099.
[41] X. Cao, R. Prozorov, Yu. Koltypin, G. Kataby, I. Felner, A. Gedanken, *J. Mater. Res.* **1997**, *12*, 402.
[42] X. Cao, Yu. Koltypin, R. Prozorov, I. Felner, A. Gedanken, *J. Mater. Chem.* **1997**, *7*, 1007.
[43] S. Avivi, I. Felner, I. Novik, A. Gedanken, *Biochim. Biophys. Acta Gen. Subj.* **2001**, *1527*, 123.
[44] F. J-J. Toublan, S. Boppart, K. S. Suslick, *J. Am. Chem. Soc.* **2006**, *128*, 3472.
[45] T. Peters, *All About Albumin: Biochemistry, Genetics, and Medical Applications*, Academic Press, New York, **1996**.
[46] S. Avivi, A. Gedanken, *Biochem. J.* **2002**, *366*, 705.
[47] L. Lins, R. Brausser, *FASEB J.* **1995**, *9*, 535.
[48] E. M. Dibbern, F. J-J. Toublan, K. S. Suslick, *J. Am. Chem. Soc.* **2006**, *128*, 6540.
[49] K. J. Liu, M. W. Grinstaff, J. J. Jiang, K. S. Suslick, H. M. Swartz, W. Wang, *Biophys. J.* **1994**, *67*, 896.
[50] A. G. Webb, M. Wong, K. J. Kolbeck, R. L. Magin, K. S. Suslick, *J. Magn. Reson. Imaging* **1996**, *6*, 675.
[51] T. M. Lee, A. L. Oldenburg, S. Sitafalwalla, D. L. Marks, W. Luo, F. J.-J. Toublan, K. S. Suslick, S. A. Boppart, *Opt. Lett.* **2003**, *28*, 1546.
[52] T. Shiomi, T. Tsunoda, A. Kawai, H. Chiku, F. Mizukami, K. Sakaguchi, *Chem. Commun.* **2005**, 5325.
[53] P. B. Stathopulos, G. A. Scholz, Y. M. Hwang, J. A. Q. Rumfeldt, J. R. Lepock, E. M. Meiering, *Protein Sci.* **2004**, *13*, 3017.
[54] Y. C. Han, S. P. Li, X. Y. Wang, X. Y. Cao, L. Jia, J. H. Li, *Colloid Polym. Sci.* **2005**, *284*, 203.
[55] M. T. Zhong, X. W. Ming, P. W. Su, Q. K. Ju, *Ultrason. Sonochem.* **2004**, *11*, 399.

Published online: February 27, 2008

